Evolution of the mating type locus with suppressed recombination

Zena Hadjivasiliou[1,2,3] and Andrew Pomiankowski[2,3]

14th December 2018

Abstract

The two partners required for sexual reproduction are rarely the same. This pattern extends to species which lack sexual dimorphism yet possess self incompatible gametes determined at mating type regions of suppressed recombination, likely precursors of sex chromosomes. In this work we investigate the role of cellular signaling in the evolution of mating types. We develop a model of ligand and receptor dynamics in individual cells, and identify key factors that determine the capacity of cells to send and receive signals. The model identifies the conditions that lead to the evolution of gametes that produce ligand and receptor in an asymmetric manner and shows how these are affected by recombination. Given that the recombination rate can evolve, the same conditions that favor asymmetric signaling also favor tight linkage of ligand and receptor loci in distinct linkage groups. These results suggest that selection for asymmetric signaling between gametes was the first step in the evolution of non-recombinant mating type loci, paving the road for the evolution of anisogamy and sexes.

keywords: mating types, sex chromosomes, recombination, linkage, cell signaling, sexes

affiliations: 1) Department of Biochemistry, University of Geneva, Geneva, Switzerland 2) CoMPLEX, Centre for Mathematics and Physics in the Life Sciences and Experimental Biology, Uni-

versity College London, Gower Street, London, UK, 3) Department of Genetics, Evolution and Environment, University College London, Gower Street, London, UK

author for correspondence: zena.hadjivasiliou@unige.ch

1 Introduction

Sex requires the fusion of two cells. With few exceptions, the sexual process is asymmetric with partnering cells exhibiting genetic, physiological or behavioral differences. The origins of sexual asymmetry in eukaryotes trace back to unicellular organisms with isogametes lacking any size or mobility difference in the fusing cells [1, 2, 3, 4, 5, 6] . Isogamous organisms are divided into genetically distinct mating types, determined by several mating type specific genes that reside in regions of suppressed recombination [7, 8, 9, 10]. The morphologically identical gametes mate disassortatively, scarcely ever with members of the same mating type. This arrangement poses a paradox as it restricts the pool of potential partners to those of a different mating type, introducing a major cost [4].

Several hypotheses have been proposed to explain the evolution of isogamous mating types [11, 12, 13]. Mating types could serve as a restrictive mechanism preventing matings between related individuals thereby avoiding the deleterious consequences of inbreeding [14, 15, 16]. Another idea is that mating types facilitate uniparental inheritance of mitochondria, which leads to improved contribution of the mitochondrial genome to cell fitness [17, 18, 19, 20, 21, 22, 23, 24]. Both hypotheses have been studied extensively and offer compelling arguments. Nevertheless, the existence of several species where inbreeding [13, 12] or biperental inheritance of mitochondria [25, 12] are the rule but nonetheless maintain mating types, indicates that these ideas may not alone explain the evolution of mating types.

An alternative hypothesis is that mating types are determined by the molecular system regulating gamete interactions [26, 27, 4]. Such interactions dictate the success of mating by guiding partner attraction and recognition and the process of cell fusion, and have been shown to be more

efficient when operating in an asymmetric manner [26]. For example, diffusible molecules are often employed as signals that guide synchronous entry to gametogenesis or as chemoatractants [28, 29, 30, 31]. Secreting and sensing the same diffusible molecule impedes the ability of cells to accurately detect external signals and makes partner finding many-fold slower [26]. In addition, secreting and detecting the same molecule in cell colonies can prevent individuals responding to signals from others [32]. Our previous review revealed that sexual signaling and communication in isogamous species are universally asymmetric [27]. This applies throughout the sexual process from signals that lead to gametic differentiation, to attraction via diffusible pheromones and interactions via surface bound molecules during cell fusion [27].

In this work we take this analysis further by explicitly considering ligand-receptor interactions between and within cells. We directly follow the dynamics of ligand and receptor molecules that are surface bound and determine the conditions under which the production of within cell ligand-receptor pairs impedes between cell communication. We use this framework to explore the evolution of gametic interactions and show that asymmetric signaling roles and tight linkage between receptor and ligand loci both evolve due to selection for robust intercellular communication and quick mating. Our findings demonstrate that the evolution of mating type loci with suppressed recombination can be traced back to the fundamental selection for asymmetric signaling during sex.

2 Theoretical set-up

Consider a population where cells encounter one another at random and can mate when in physical contact. Interactions between cells leading to successful mating are dictated by a ligand-receptor pair. In this work we assume that the ligand-receptor interactions only operate locally. Receptors remain bound to the cell surface and ligands only undergo localized diffusion (Fig. 1) as is the case in several yeast and other unicellular eukaryotes [33, 29, 34, 35]. The following equations describe

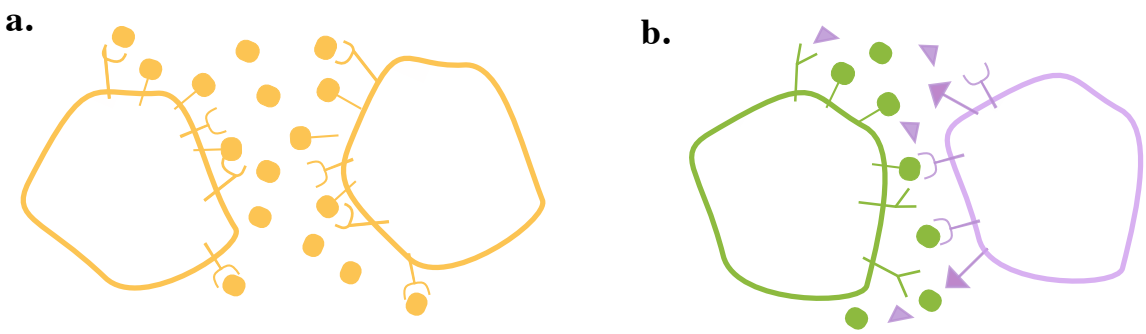

Figure 1: **Gametes communicate through ligand and receptor molecules.** The ligand can be either membrane bound or released in the local environment. (a) When the interacting cells produce ligand and receptor symmetrically, the ligand will bind to receptors on its own membrane as well as those on the other cell. This may impair intercellular signaling. (b) Producing the ligand and receptor in an asymmetric manner resolves this issue.

the concentration of free ligand L, free receptor R and bound ligand LR within a single cell

$$\frac{d[L]}{dR} = \nu_L - k^+[R][L] + k^-[LR] - \gamma_L[L], \tag{1}$$

$$\frac{d[R]}{dR} = \nu_R - k^+[R][L] + k^-[LR] - \gamma_R[R], \tag{2}$$

$$\frac{d[LR]}{dR} = k^+[R][L] - k^-[LR] - \gamma_{LR}[LR]. \tag{3}$$

ν_L and ν_R describe the rate of production of the ligand and receptor respectively. γ_L, γ_R, and γ_{LR}, are the degradation rate of the ligand, receptor and bound complex respectively. The terms k^+ and k^- are the binding and unbinding rates that determine the affinity of the ligand to its receptor within a single cell. We can solve Eq. (1-3) by setting the dynamics to zero to obtain the amount of free and ligand and receptor ($[L]^*$, $[R]^*$) and bound complex at steady state ($[LR]^*$). ,

$$[L]^* = \frac{k^+\gamma_{LR}(\nu_L - \nu_R) - k^-\gamma_L\gamma_R - \gamma_L\gamma_R\gamma_{LR} + \Delta}{2k^+\gamma_L\gamma_{LR}}, \tag{4}$$

$$[R]^* = \frac{k^+\gamma_{LR}(\nu_R - \nu_L) - k^-\gamma_L\gamma_R - \gamma_L\gamma_R\gamma_{LR} + \Delta}{2k^+\gamma_R\gamma_{LR}}, \tag{5}$$

$$[LR]^* = \frac{k^+\gamma_{LR}(\nu_R + \nu_L) + k^-\gamma_L\gamma_R + \gamma_L\gamma_R\gamma_{LR} - \Delta}{2k^+\gamma_{LR}^2}, \tag{6}$$

Where Δ is given by,

$$\Delta = \sqrt{(k^-\gamma_L\gamma_R + \gamma_{LR}(\gamma_L\gamma_R + k^+\gamma_{LR}(\nu_R + \nu_L)))^2 + 4k^+\gamma_L\gamma_R\gamma_{LR}(k^- + \gamma_{LR})\nu_R}. \tag{7}$$

The likelihood of a successful mating between two cells depends not just on partner signaling levels but also on how accurately the cells can compute the signal produced by their partner. Binding of ligand and receptor originating from the same cell can obstruct this interaction. To capture this, we define the strength of the incoming signal for cell$_1$ when it interacts with cell$_2$ as,

$$W_{1,2} = k_b[L_2]^*[R_1]^* \left(1 - \frac{[LR_1]^*}{[LR_1]^* + k_b[L_2]^*[R_1]^*}\right)^n, \tag{8}$$

where subscripts denote concentrations in cell$_1$ and cell$_2$, and the parameter k_b determines the affinity of the ligand and receptor between cells. If k_b is the same as the affinity of receptor and ligand within cells, then $k_b = \frac{k^+}{k^-}$. We also consider cases where $k_b \neq \frac{k^+}{k^-}$, for example, when ligand interacts differently with receptors on the same as opposed to a different cell [36, 37].

The cost of self-signaling is determined by n. When $n = 0$, $W_{1,2}$ reduces to $k_b[R_1]^*[L_2]^*$ with the incoming signal dependent on the concentration of ligand produced by cell$_2$ and receptor produced by cell$_1$. This corresponds to a case where self-binding does not lead to activation but only causes an indirect cost through the depletion of available ligand and receptor molecules. When $n \geq 1$, binding within a cell leads to some form of activation that interferes with between cell signaling,

imposing a cost in evaluating the incoming signal. Higher values for n correspond to more severe costs due to self-binding.

The likelihood that two cells successfully mate (P) depends on the quality of their interaction given by,

$$P = \frac{W_{1,2}W_{2,1}}{K + W_{1,2}W_{2,1}}. \tag{9}$$

Eq. (9) transforms the signaling interaction into a mating probability. For the analysis that follows, we choose large values of K so that P is far from saturation and depends almost linearly on the product $W_{1,2}W_{2,1}$. In summary, the probability that two cells mate is defined by the production and degradation rates of the ligand and receptor molecule, and the binding affinities between and within cells.

2.1 Evolutionary model

To explore the evolution of signaling roles, we simplify the model by assuming that the degradation rates $\gamma_L, \gamma_R, \gamma_{LR}$ are constant and equal to γ, and only investigate mutations that quantitatively modify the ligand and receptor production rates. Consider a finite population of N haploid cells where loci that control ligand and receptor production evolve continuously. The ligand and receptor production rates of cell$_i$ is denoted by (ν_{L_i}, ν_{R_i}) . We also consider different versions of the ligand and its receptor so that that the organism has two ligand-receptor pairs, the second being designated (l, r). We assume (L, R) and (l, r) to be mutually incompatible, so the binding affinity is zero between l and R, and between L and r. Each cell has a (L, R) and (l, r) state, which are subject to mutational and evolutionary pressure as described below. $W_{1,2}$ is re-defined as the summation of the interactions of these two ligand-receptor pairs,

$$W_{1,2} = k_b[L_2]^*[R_1]^* \left(1 - \frac{[LR_1]^*}{[LR_1]^* + k_b[L_2]^*[R_1]^*}\right)^n + k_b[l_2]^*[r_1]^* \left(1 - \frac{[lr_1]^*}{[lr_1]^* + k_b[l_2]^*[r_1]^*}\right)^n. \tag{10}$$

Again for the sake of simplicity, the ligand-receptor affinities are set to be the same between and within cells (i.e. k^+, k^- and k_b), and for each ligand-receptor pair. A cell undergoes mutation that changes $\nu'_{L_i} = \nu_{L_i} + \epsilon$ with $\epsilon \sim N(0, \sigma)$ with probability μ. The same mutational process occurs for all ligand and receptor production rates. We assume that mutation occurs independently at different loci and that there is a maximum capacity for the ligand and receptor production, so that $\nu_L + \nu_l$ and $\nu_R + \nu_r$ cannot exceed 1.

The evolution of ligand-receptor production rates is governed by the likelihood that cells pair and produce offspring. Pairs of haploid cells are randomly sampled (to reflect random encounters) and mate with probability P defined in Eq. (9). Cells failing to mate are returned to the pool of unmated individuals. The process is repeated until M cells have mated. Each mated pair produces 2 haploid offspring so the population size shrinks from N to M. The population size is restored back to N by sampling with replacement. Initially, recombination is not allowed between the genes controlling ligand and receptor production but then is considered in a later section.

3 Results

3.1 Dependence of gamete interactions on physical parameters

The strength of an incoming signal $W_{1,2}$ depends on the concentration of free receptor in cell$_1$ and free ligand in cell$_2$, and the cost of self-binding (n) (Eq. 10 and Fig. S1). The concentrations are governed by the production and degradation rates and self-binding. For low degradation rates (γ small), the removal of available molecules is dominated by self-binding (k^+) (Eq. 1 and 2 and Fig. 2a, b). In this case, the negative effect of within cell binding is amplified. At the same time, a lower degradation rate leads to higher levels of ligand and receptor (Fig. 2a) even if the relative drop of free ligand and receptor is steeper as k^+ increases (Fig. 2b). As a consequence, the ability of a cell to generate a strong signal and read incoming signals, can change drastically when the pair of interacting cells produce the ligand and receptor symmetrically (e.g. ($\nu_{R_1} = \nu_{L_1} = \nu_{R_2} = \nu_{L_2} = 1$) for both cells) rather than in a asymmetric manner (e.g. ($\nu_{R_1} = 1, \nu_{L_1} = 0, \nu_{R_2} = 0, \nu_{L_2} = 1$). The

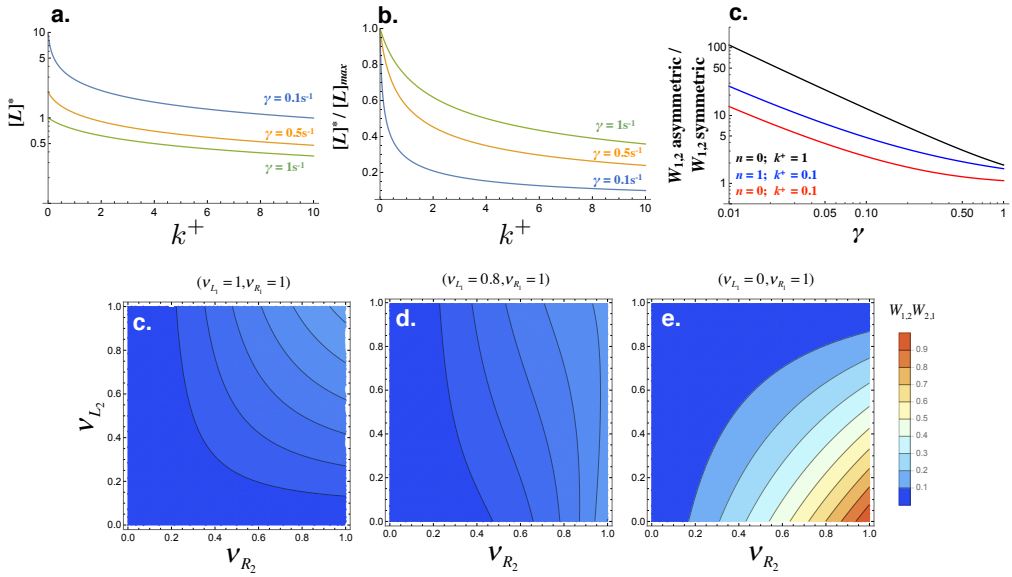

Figure 2: **Signaling interactions between mating cells can be severely impaired due to ligand-receptor interactions in the same cell**. (a) The amount of free ligand in individual cells at steady state $[L]^*$ and (b) normalized amount of free ligand at steady state $[L]^*/[L]_{max}$ varies with the intracellular binding rate k^+ and degradation rate γ. (c) The relative amount of incoming signal W_{12} for a cell that produces ligand and receptor asymmetrically versus symmetrically decreases with the degradation rate $\gamma$and weaker binding k^+. (d-f) The product of the incoming signal of two interacting cells $W_{12}W_{21}$ (determining the likelihood of a successful mating interaction) varies with ligand and receptor production rates in cell$_1$ and cell$_2$. Other parameters used in the simulations are given in the Supplemental Material.

fold-increase in $W_{1,2}$ is large even when self-binding confers no cost ($n = 0$), while larger values for n ramp up the costs (Fig. 2c). If cells produce the ligand and receptor asymmetrically, self-binding ceases to be a problem in receiving incoming signals.

Although the strength of the incoming signal ($W_{1,2}$) may improve when the interacting cells produce the ligand and receptor asymmetrically, this need not be the case. Take for example cell$_1$ that produces the ligand and receptor symmetrically $(\nu_R, \nu_L, \nu_r, \nu_l) = (1, 1, 0, 0)$. The interaction between cell$_1$ and cell$_2$ is optimal when cell$_2$ also produces the ligand and receptor symmetrically (Eq. 8 and Fig. 2b). Increasing the asymmetry in signaling in cell$_2$ by producing less ligand L and more ligand l, for example, will provide little advantage simply because cell$_2$ does not produce the appropriate receptor r. If on the other hand cell$_1$ shows some asymmetry so that $(\nu_R, \nu_L, \nu_r, \nu_l) = (a, 1, 1-a, 0)$ an asymmetry in cell$_2$ (in the opposite direction) begins to convey benefits (Fig. 2c-d). It follows that asymmetric signaling becomes beneficial once cells that exhibit some asymmetry in opposite directions begin to evolve and encounter one another.

3.2 Evolution of mating types with asymmetric signaling roles

To explore the evolution of asymmetry, we follow mutations that alter the relative production of two mutually incompatible types of ligand and receptor (L, R) and (l, r). To ease understanding, the population asymmetry s in the production of ligand and receptor is measured,

$$s = \frac{1}{2N} \sum_{i=1}^{N} \left(|\nu_{L_i} - \nu_{R_i}| + |\nu_{l_i} - \nu_{r_i}| \right). \tag{11}$$

There is no asymmetry ($s = 0$) if cells produce the two types of ligand and receptor equally (i.e. $(\nu_R, \nu_L,\ \nu_r, \nu_l) = (a, a, 1-a, 1-a)$, for constant a), and full asymmetry ($s = 1$) when cells adopt polarized roles (i.e. $(\nu_R, \nu_L, \nu_r, \nu_l) = (1, 0, 0, 1)$ or $(0, 1, 1, 0)$).

Starting from a population where all cells are symmetric producers of only one ligand and receptor, $(\nu_R, \nu_L, \nu_r, \nu_l) = (1, 1, 0, 0)$, the population evolves to one of two equilibria (Fig. 3a). E_1 where $s^* \approx 0$ and all cells produce the ligand and receptor symmetrically $(\nu_R, \nu_L, \nu_r, \nu_l) \approx (1, 1, 0, 0)$

or E_2 where $s^* \approx 1$ and the population is divided into ligand and receptor producing cells, with equal frequencies of $(\nu_R, \nu_L, \nu_r, \nu_l) \approx (1,0,0,1)$ and $(\nu_R, \nu_L, \nu_r, \nu_l) \approx (0,1,1,0)$ (Fig. 3b, c). Equilibria with intermediate values of s^* are not found. The exact production rates at E_1 and E_2 exhibit some degree of noise due to mutation and finite population size (Fig. 3b, c). For individual cells at steady state, cells with high ν_R have insignificant ν_L and the same for ν_r and ν_l. Furthermore, cells that produce the R receptor maximally do not produce the r receptor and vice versa (Fig. 3c; the same is true for ν_L and ν_l, not shown), confirming that $s^* \approx 1$ captures a fully asymmetric steady state.

The stability of E_1 and E_2 depends on key parameters that determine the strength of self-binding and signaling interactions between cells. E_1 is stable and no asymmetry evolves when k^+ (the intracellular ligand-receptor binding coefficient) is small (Fig. 3d). In this case, the concentration of self-bound ligand-receptor complex is small (Eq(6)) and there is little cost of self-signaling (Eq(8)), so there is weak selection in favor of asymmetry. The opposite is true for larger values of k^+, as self-binding now dominates and restricts between cell signaling, promoting the evolution of asymmetry (Fig. 3d). The switch from E_1 to E_2 occurs at a smaller value of k^+ when the degradation rate (γ) is decreased (Fig. 3d), as the effective removal of free ligand and receptor depends more strongly on intercellular binding (Fig. 2a, b).

Another important consideration is the relative strength of signaling within and between cells, given by k^+/k^- and k_b respectively. For example, the threshold value of the within cell binding rate beyond which symmetric signaling (E_1) evolves to to asymmetric signaling (E_2, Fig. 3d) increases when k_b becomes much larger than k^+/k^- (Fig. 3e). Furthermore, this threshold value is smaller for larger values of n indicating that asymmetric signaling is more likely to evolve when the cost for self-signaling is higher (larger n, Fig. 3e). However, asymmetric signaling can evolve even when self-binding carries no cost ($n = 0$) as high rates of self-binding can restrict the number of ligand and receptor molecules free for between cell interactions (Fig. 3e).

If the initial values are arbitrary (e.g. $(\nu_R, \nu_L, \nu_r, \nu_l) = (a, b, 1-a, 1-b)$), the two equilibria have domains of attraction, with a region of separation dependent on the stochasticity of the mutational input and frequency-dependent selection favoring one of the two equilibria (Fig. 3f). Interestingly,

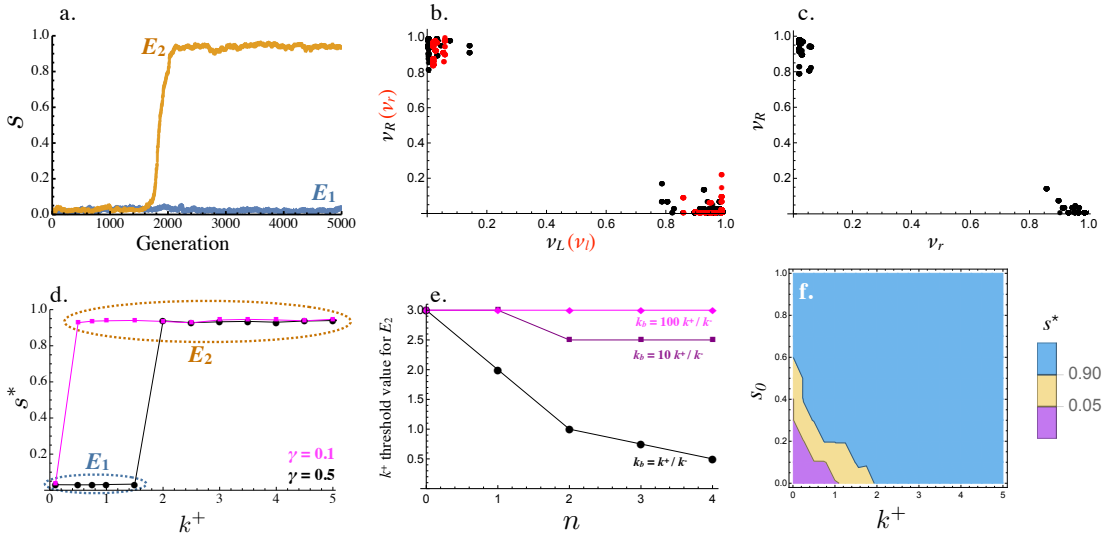

Figure 3: **Evolution of asymmetric signaling roles and self-incompatible mating types.** (a) The evolution of signaling asymmetry ($s = 0$ no asymmetry, $s = 1$ full asymmetry) over time. Two steady states (E_1 and E_2) are found as described in the main text. (b) Production rates of individual cells in the population for the receptor-ligand pairs $L-R$ (black) and $l-r$ (red) at E_2. (c) Production rates for the two receptor types R and r for individual cells at E_2. (d) Steady state signaling asymmetry s^* against the intracellular binding rate k^+. (e) Threshold value of k^+, beyond which E_2 becomes stable against E_1, plotted versus n (cost of self-binding). The relationship is shown for different values of k_b (strength of between cell signaling) relative to k^+/k^- (strength of within cell signaling) (f): The steady state value for s^*, plotted versus the initial value s_0 and k^+. Plots are averaged at the steady state over 20 repeats. s^* values away from 0 or 1 reflect stochastic outcomes where the population evolves to either E_1 or E_2. Other parameters used in simulations detail in the Supplemental Material.

E_2 appears to be stable for very small values of k^+. This implies that strong selection for asymmetric signaling is required to allow the system to evolve from E_1 to E_2. But as the population approaches E_2 it becomes attracted to it even if selection for asymmetry becomes weaker (i.e. E_2 is attractive when there is an initial asymmetry even for small values of k^+, Fig. 3f). Along a similar logic, higher mutation rates mean that E_2 evolves more easily as meetings between cells that mutate in opposite directions become more likely before they become lost by drift when rare (Fig. S2).

3.3 Effects of recombination

The results above assume that the loci controlling ligand and receptor production are tightly linked which prevents the production of deleterious combinations following meiosis. Recombination is

a minor problem at the E_1 equilibrium which is monomorphic (except for mutational variation). But it is likely to be a problem at the polymorphic E_2 equilibrium. At E_2, mating between $(\nu_R, \nu_L, \nu_r, \nu_l) = (1,0,0,1)$ and (0, 1, 1, 0) cells generates non-asymmetric recombinant ligand-receptor combinations, either $(1,1,0,0)$ or $(0,0,1,1)$.

Allowing recombination for values of k^+ and n that previously led to E_2, s^* evolves away from unity in proportion to the recombination rate, r (Fig. 4a, b). For low recombination rates ($r \leq 0.1$), the population largely consists of equal frequencies of $(1,0,0,1)$ and (0, 1, 1, 0) cells, producing the ligand and receptor asymmetrically. A smaller percentage of recombinant cells produce conspecific pairs of ligand and receptor $(1,1,0,0)$ and $(0,0,1,1)$ (Fig. 4b, c). Recombination in this case creates "macromutations" where 0 becomes 1 and vice versa. As the recombination rate rises ($r \geq 0.2$), the two leading cell types diverge from $(1,0,0,1)$ and (0, 1, 1, 0) towards (1 - ϵ_1, ϵ_2, ϵ_3, 1-ϵ_4) and (ϵ_5, 1 - ϵ_6, 1 - ϵ_7, ϵ_8) where the ϵ_i are below 0.5 but greater than zero Fig. 4d). Higher recombination rates ($r \geq 0.3$) pushes $s^* = 0.5$ at E_2 (Fig. 4b). Here, there is a predominance of $(1,0.5,0,0.5)$ and $(0,0.5,1,0.5)$ cells at equal frequencies. This arrangement is robust to recombination since the receptor locus is fixed at $(\nu_R, \nu_r) = (0.5, 0.5)$ and the ligand locus is either at $(\nu_L, \nu_l) = (1,0)$ or $(0,1)$. So pairing between these two cell types results in $(1,0.5,0,0.5)$ and $(0,0.5,1,0.5)$ offspring, whether recombination occurs or not. Note that this arrangement maintains some degree of asymmetry even with free recombination ($r = 0.5$). Even though both cell types produce both receptors, they produce the ligand asymmetrically. Cells on average are more likely to mate successfully between rather than within the two types of cells .

Similarly as in the case of no recombination, the steady state depends on initial conditions (Fig. 4f). When the initial values are arbitrary (i.e. $(\nu_R, \nu_L, \nu_r, \nu_l) = (a, b, 1-a, 1-b)$) then E_1 becomes attractive for smaller k^+ values (Fig. 4f).

3.4 Evolution of linkage

In the analysis above, recombination between the ligand and receptor loci is fixed at a non-zero value. However, the recombination rate itself can evolve. Let r undergo mutation at rate μ_r so that

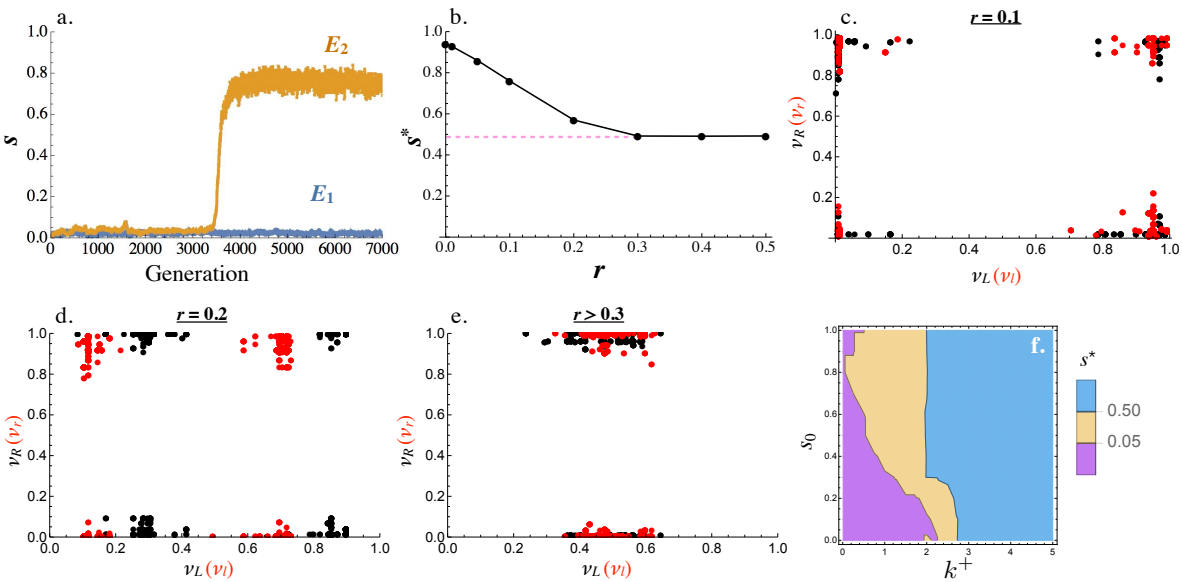

Figure 4: **Recombination impacts E_2.** (a) The evolution of s (signaling asymmetry) over time given a fixed recombination rate $r = 0.1$. (b) Steady state ss^* varies with the recombination rate. (c-e) Production rates of individual cells in the population for receptor-ligand pairs $L-R$ (black) and $l-r$ (red) for recombination rates (c) , $r = 0.1$ (d) 0.2 and (e) > 0.3. (f) The steady state value for ss^*, given a recombination rate $r = 0.2$, plotted versus the initial $s$value s_0 and k^+ averaged over 20 repeats. s^* values away from 0 or 0.5 reflect a stochastic outcome. Other parameters used in simulations detail in the Supplemental Material.

$r' = r + \varepsilon_r$ with $\varepsilon_r \sim N(0, \sigma_r)$ at each generation. In a diploid zygote, the rate of recombination is given by the average of the two recombination alleles, r_1 and r_2, carried by the mating cells. In this way, the recombination rate evolves together with the ligand and receptor production rates. We start with maximal recombination rate $r = 0.5$ and $(\nu_R, \nu_L, \nu_r, \nu_l) = (1, 1, 0, 0)$ for all cells and allow the recombination rate to evolve by drift for 1000 generation before we introduce mutation in the ligand and receptor loci.

The recombination rate evolves to $r^* = 0$ whenever E_2 is stable in the non-recombination analysis. Tight linkage between receptor and ligand genes is favored when asymmetric signaling is adaptive (Fig. 5a). Furthermore, asymmetric signaling roles coevolve together with the recombination rate. The evolved trajectories of s and r depend on the strength of selection for asymmetric signaling. For example, when k^+ is large ($k^+ = 10$), signal asymmetry rapidly evolves; s moves away from 0 and this is followed by a sharp drop in the recombination rate (Fig. 5b). Eventually the population evolves asymmetric signaling roles (s in orange, Fig. 5b) and tight linkage (r in blue, Fig. 5b). These dynamics are similar when k^+ is smaller ($k^+ = 3$, Fig. 5c) and selection for asymmetry is weaker. However, it now takes longer for the asymmetric types to co-evolve (Fig. 5c). When selection for asymmetric signaling is even weaker ($k^+ = 1$, fig. 5d), no asymmetry evolves (s remains at zero) and the recombination rate fluctuates randomly as one would expect in the case of a neutral allele.

4 Discussion

Explaining the evolution of mating types in isogamous organisms constitutes a major milestone in understanding the evolution of anisogamy and sexes [1, 3]. Mating type identity is determined by a number of genes that reside in regions of suppressed recombination and code for ligands and receptors that guide partner attraction and recognition, as well as genes that orchestrate cell fusion and postzygotic events [27, 8, 13, 12]. In this work we show that an asymmetry in ligand and receptor production evolves as a response to selection for robust gamete communication and

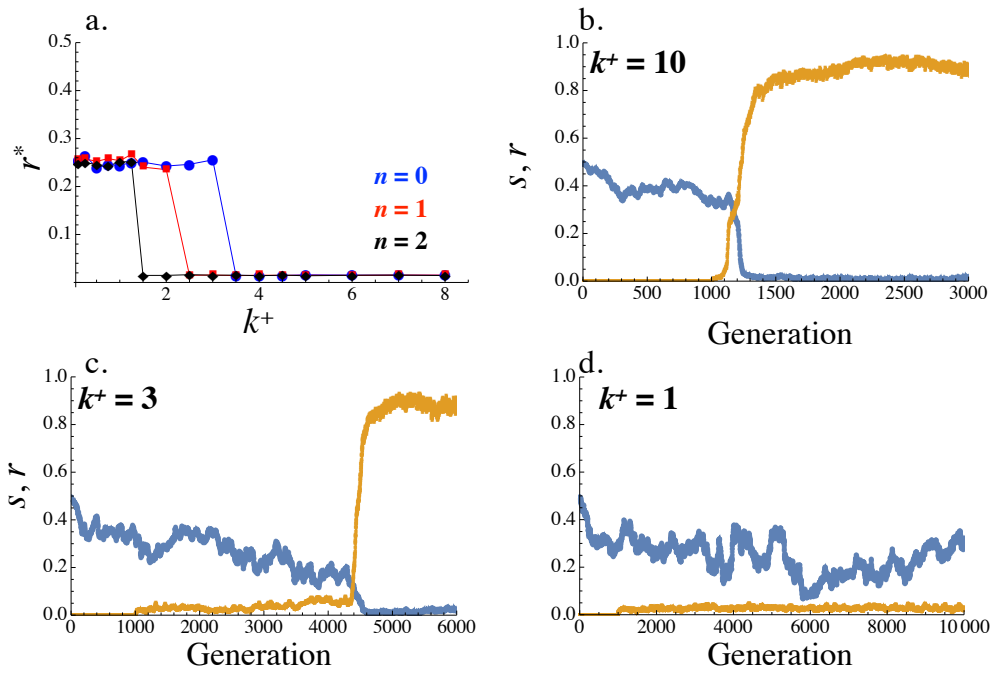

Figure 5: **The steady state recombination rate r^* co-evolves with the ligand and receptor production rates.** (a) Averaged across the population, r^* varies with k^+ (within cell binding rate) and $n = 0, 1, 2$ (cost of self-binding). Evolution trajectories of s (orange) and r (blue) over time for (b) $k^+ = 10$, (c) $k^+ = 3$ and (d) $k^+ = 1$. The recombination rate r was allowed to evolve alone for 1000 generations, following which mutation at the ligand and receptor loci was introduced. Other parameters used in simulations are given in the Supplemental Material.

swift mating. Furthermore, the same conditions favoring asymmetric signaling select for tight linkage between the receptor and ligand genes. Our findings indicate that selection for asymmetric signaling roles are likely to have played a key role in the early evolution of gamete differentiation and identity.

We investigated the evolution of mating type roles by considering two types of ligand and receptor in individual cells. Gene duplication followed by mutation is a well established route to novelty evolution [38, 39, 40], and could explain the co-existence of two pairs of ligand and receptor in our system. Alternatively, individual cells could produce multiple ligand and receptors which evolve independently, as is the case in some basidiomycete fungi [41]. The production rate of the two types of ligand (and receptor) in our system is subject to mutation and selection so that the amount of expressed ligand (and receptor) of each kind is modulated quantitatively. In this way we were able to explicitly express the likelihood of mating as a function of the amount of free and bound molecules on the cell membrane and the ability of cells to accurately read their partner's signal. This framework also allowed us to quantitatively follow the evolution of ligand and receptor production in mating cells for the first time.

We found that the ligand-receptor binding rate within a cell (k^+) is key in the evolution of asymmetric signaling roles (Fig. 3d-e). k^+ holds an important role because it dictates the rate at which free ligand and receptor molecules are removed from the cell surface. In addition, k^+ determines the amount of intracellular signal that interferes with the ability of cells to interpret incoming signal. Although in theory cells could avoid self-binding (by reducing k^+ to zero), there is likely to be a strong association of the within-cell and between-cell binding affinities. So reductions in k^+ are likely to have knock-on costs in reducing k_b as well. An extreme example is the case of locally diffusible signals (Fig. 1), such as those used by ciliates and yeasts to stimulate and coordinate fusion [29, 42]. Here binding affinities between and within cells are inevitably identical (since the ligand is not membrane bound). Work in yeast cells has shown that secreted ligands utilized for intercellular signaling during sex are poorly read by cells that both send and receive the same ligand [32]. In the case of strictly membrane bound molecules avoiding self-binding could

also be an issue as it requires a ligand and receptor pair that bind poorly within a cell without compromising intercellular binding. For example, choosy budding yeast gametes (which are better at discriminating between species) take longer to mate [43]. It would be interesting to further study these trade-offs experimentally.

We never observed the co-existence of a symmetric "pansexual" type with asymmetric self-incompatible types. The two steady states consist of either a pansexual type or two mating types with asymmetric signaling roles. This follows from the requirement for strong selection to initiate evolution towards asymmetric signaling roles, and could explain why the co-existence of mating types with pansexuals is rare in natural populations [11, 12]. This is in contrast to previous models were pansexual types were very hard to eliminate due to negative frequency dependent selection [16, 44, 24]. For example, in the case of the mitochondrial inheritance model, uniparental inheritance raises mean population fitness, not only in individuals that carry genes for uniparental inheritance but also for pansexual individuals (benefits "leak" to biparental individuals) [24, 45]. A similar pattern is seen with inbreeding avoidance because the spread of self-incompatibility reduces the population mutation load, and so reduces the need for inbreeding avoidance [16]. These dynamics are reversed in the present model where there is positive frequency dependent selection. The spread of asymmetric signalers generates stronger selection for further asymmetry (Fig. 3f). This also occurs when there is recombination (Fig. 4f). Even though recombination between the two asymmetric types generates symmetric recombinant offspring, these are disfavored and eliminated by selection. These observations suggest that the mitochondrial inheritance and inbreeding avoidance models are unlikely to generate strong selection for suppressed recombination which is the hallmark of mating types. Finally, it would be interesting to explore how the reinstatement of recombination could be a route back to homothallism which is a state derived from species with mating types [12].

Mating type identity in unicellular eukaryotes is determined by mating type loci that typically carry a number of genes [27, 11]. Suppressed recombination at the mating type locus is a common feature across the evolutionary tree [8]. Our work predicts the co-evolution of mating type specific

signaling roles and suppressed recombination with selection favoring linkage between loci responsible for signaling and an asymmetry in signaling roles (Fig. 5). This finding suggests that selection for asymmetric signaling could be the very first step in the evolution of tight linkage between genes that control mating type identity. In yeasts, the only genes in the mating type locus code for the production of ligand and receptor molecules [29]. These then trigger a cascade of other signals downstream that also operate asymmetrically. Evidence across species suggests that mating types loci with suppressed recombination are precursors to sex chromosomes [46, 47]. In this way our work provides crucial insights about the origin of sex chromosomes.

The framework developed here could be used together with recent efforts to understand numerous features of mating type evolution. For example, opposite mating type gametes often utilize diffusible signals to attract partners [48, 49]. The inclusion of long range signals such as those used in sexual chemotaxis will provide further benefits for asymmetric signaling roles and mating types [26]. Furthermore the number of mating types varies greatly across species and is likely to depend on the frequency of sexual reproduction and mutation rates [50]. Signaling interactions between gametes could also play a role in determining the number of mating types and reducing their number to only two in many species [27]. Other important features such as the mechanism of mating type determination [12, 51] and stochasticity in mating type identity [52, 53, 54] could also be understood in light of this work.

Taken together our findings suggest that selection for swift and robust signaling interactions between mating cells can lead to the evolution of self-incompatible mating types with non-recombinant mating type loci. We conclude that the fundamental selection for asymmetric signaling between mating cells was likely the very first step in the evolution of sexual asymmetry and paved the way for the evolution of anisogamy, sex chromosomes and sexes.

References

[1] J. Lehtonen, H. Kokko, and G. A. Parker. What do isogamous organisms teach us about sex and the two sexes? *Philosophical Transactions of the Royal Society B: Biological Sciences*, 371(1706):20150532, 2016.

[2] G. A. Parker, R. R. Baker, and V. G. F. Smith. The origin and evolution of gamete dimorphism and the male-female phenomenon. *Journal of Theoretical Biology*, 36(3):529–553, 1972.

[3] J. R. Randerson and L. D. Hurst. The uncertain evolution of the sexes. *Trends in Ecology and Evolution*, 16(10):571–579, 2001.

[4] R. F. Hoekstra. The evolution of sexes. In S. C. Stearns, editor, *The evolution of sex and its consequences*, pages 59–91. Birkhauser Verlag, Basel, 1987.

[5] G. Bell. The evolution of anisogamy. *Journal of Theoretical Biology*, 73(2):247–270, 1978.

[6] B. Charlesworth. The population genetics of anisogamy. *Journal of Theoretical Biology*, 73(2):347–57, 1978.

[7] S. Branco, H. Badouin, R C. Rodríguez de la Vega, J. Gouzy, F. Carpentier, G. Aguileta, S. Siguenza, J. T. Brandenburg, M. A. Coelho, M. E. Hood, and T. Giraud. Evolutionary strata on young mating-type chromosomes despite the lack of sexual antagonism. *Proceedings of the National Academy of Sciences*, 114(27):7067–7072, 2017.

[8] S. Branco, F. Carpentier, R .C. R. De La Vega, H. Badouin, A. Snirc, S. Le Prieur, M. A. Coelho, D. M. De Vienne, F. E. Hartmann, D. Begerow, M. E. Hood, and T. Giraud. Multiple convergent supergene evolution events in mating-type chromosomes. *Nature Communications*, 9(1):2000, 2018.

[9] S. Ahmed, J. M. Cock, E. Pessia, R. Luthringer, A. Cormier, M. Robuchon, L. Sterck, A. F. Peters, S. M. Dittami, E. Corre, M. Valero, J. M. Aury, D. Roze, Y. Van De Peer, J. Bothwell,

G. A. B. Marais, and S. M. Coelho. A haploid system of sex determination in the brown alga *ectocarpus sp*. *Current Biology*, 24(17):1945–1957, 2014.

[10] J. A. Fraser, S. Diezmann, R. L. Subaran, A. Allen, K. B. Lengeler, F. S. Dietrich, and J. Heitman. Convergent evolution of chromosomal sex-determining regions in the animal and fungal kingdoms. *PLoS Biology*, 2(12):e384, 2004.

[11] S. Billiard, M. López-Villavicencio, M. E. Hood, and T. Giraud. Sex, outcrossing and mating types: unsolved questions in fungi and beyond. *Journal of Evolutionary Biology*, 25(6):1020–38, 2012.

[12] S. Billiard, M. López-Villavicencio, B. Devier, M. E. Hood, C. Fairhead, and T. Giraud. Having sex, yes, but with whom? Inferences from fungi on the evolution of anisogamy and mating types. *Biological Reviews of the Cambridge Philosophical Society*, 86(2):421–42, 2011.

[13] N. Perrin. What uses are mating types? The "developmental switch" model. *Evolution*, 66(4):947–56, apr 2012.

[14] D. Charlesworth and B. Charlesworth. The evolution and breakdown of S-allele systems. *Heredity*, 43(1):41–55, 1979.

[15] M. K. Uyenoyama. On the evolution of genetic incompatibility systems. III. Introduction of weak gametophytic self-incompatibility under partial inbreeding. *Theoretical Population Biology*, 34(1):47–91, aug 1988.

[16] T. L. Czárán and R. F. Hoekstra. Evolution of sexual asymmetry. *BMC Evolutionary Biology*, 4(1):34, 2004.

[17] Z. Hadjivasiliou, A. Pomiankowski, R.M. Seymour, and N. Lane. Selection for mitonuclear co-adaptation could favour the evolution of two sexes. *Proceedings of the Royal Society B: Biological Sciences*, 279(1734), 2012.

[18] J. R. Christie, T. M. Schaerf, and M. Beekman. Selection against heteroplasmy explains the evolution of uniparental inheritance of mitochondria. *PLoS Genetics*, 11(4):e1005112, 2015.

[19] L. D. Hurst and W. D. Hamilton. Cytoplasmic fusion and the nature of sexes. *Proceedings of the Royal Society B: Biological Sciences*, 247(1320):189–194, 1992.

[20] L. D. Hurst. Why are there only two sexes? *Proceedings of the Royal Society B: Biological Sciences*, 263:415–422, 1996.

[21] V. Hutson and R. Law. Four steps to two sexes. *Proceedings of the Royal Society B: Biological Sciences*, 253(1336):43–51, 1993.

[22] J. R. Christie and M. Beekman. Uniparental inheritance promotes adaptive evolution in cytoplasmic genomes. *Molecular Biology and Evolution*, 34(3):677–691, 2017.

[23] I. M. Hastings. Population genetic aspects of deleterious cytoplasmic genomes and their effect on the evolution of sexual reproduction. *Genetics Research*, 59(3):215–25, 1992.

[24] Z. Hadjivasiliou, N. Lane, R. M. Seymour, and A. Pomiankowski. Dynamics of mitochondrial inheritance in the evolution of binary mating type and two sexes. *Proceedings of the Royal Society B: Biological Sciences*, 280(1769):20131920, 2013.

[25] A. J. Wilson and J. Xu. Mitochondrial inheritance: Diverse patterns and mechanisms with an emphasis on fungi. *Mycology*, 3(2):158–166, 2012.

[26] Z. Hadjivasiliou, Y. Iwasa, and A. Pomiankowski. Cell - Cell signalling in sexual chemotaxis: A basis for gametic differentiation, mating types and sexes. *Journal of the Royal Society Interface*, 12(109), 2015.

[27] Z. Hadjivasiliou and A. Pomiankowski. Gamete signalling underlies the evolution of mating types and their number. *Philosophical Transactions of the Royal Society B: Biological Sciences*, 371(1706), 2016.

[28] H. W. Kuhlmann, C. Brünen-Nieweler, and K. Heckmann. Pheromones of the ciliate *Euplotes octocarinatus* not only induce conjugation but also function as chemoattractants. *The Journal of Experimental Zoology*, 277(1):38–48, 1997.

[29] L. Merlini, O. Dudin, and S. G. Martin. Mate and fuse: how yeast cells do it. *Open Biology*, 3(3):130008, 2013.

[30] I. Maier. Gamete orientation and induction of gametogenesis by pheromones in algae and plants. *Plant, Cell & Environment*, 16:891–907, 1993.

[31] Y. Tsubo. Chemotaxis and sexual behavior in *Chlamydomonas*. *The Journal of Protozoology*, 8(2):114–121, 1961.

[32] H. Youk and W. A. Lim. Secreting and sensing the same molecule allows cells to achieve versatile social behaviors. *Science*, 343(6171):1242782, 2014.

[33] C. Cappellaro, K. Hauser, V. Mrsa, M. Watzele, G. Watzele, C. Gruber, and W. Tanner. *Saccharomyces cerevisiae* a- and α-agglutinin: characterization of their molecular interaction. *The EMBO Journal*, 10(13):4081–4088, 1991.

[34] N. F. Wilson, J. S. O'Connell, M. Lu, and W. J. Snell. Flagellar adhesion between mt+ and mt- *Chlamydomonas* gametes regulates phosphorylation of the mt+-specific homeodomain protein GSP1. *Journal of Biological Chemistry*, 274(48):34383–34388, 1999.

[35] S. S. Phadke and R. A. Zufall. Rapid diversification of mating systems in ciliates. *Biological Journal of the Linnean Society*, 98(1):187–197, 2009.

[36] Z. Hadjivasiliou, G. L. Hunter, and B. Baum. A new mechanism for spatial pattern formation via lateral and protrusionmediated lateral signalling. *Journal of the Royal Society Interface*, 13(124), 2016.

[37] L. LeBon, T. V. Lee, D. Sprinzak, H. Jafar-Nejad, and M. B. Elowitz. Fringe proteins modulate Notch-ligand cis and trans interactions to specify signaling states. *eLife*, 3:e02950, 2014.

[38] O. Susumu. *Evolution by Gene Duplication*. Springer Science, New York, 1970.

[39] J. Zhang. Evolution by gene duplication: An update. *Trends in Ecology and Evolution*, 18(6):292–298, 2003.

[40] S. Magadum, U. Banerjee, P. Murugan, D. Gangapur, and R. Ravikesavan. Gene duplication as a major force in evolution. *Journal of Genetics*, 92(1):155–161, 2013.

[41] T. J. Fowler and L. J. Vaillancourt. Pheromones and pheromone receptors in *Schizophyllum commune* mate recognition: a retrospective of a half-century of progress, and a look ahead. In J. Heitman, J. T. Kronstad, and L. A. Casselton, editors, *Sex in fungi: Molecular determination and evolutionary iImplications*, pages 301–315. American Society of Microbiology (ASM) Press, Washington D.C., 2007.

[42] M. Sugiura, H. Shiotani, T. Suzaki, and T. Harumoto. Behavioural changes induced by the conjugation-inducing pheromones, gamone 1 and 2, in the ciliate *Blepharisma japonicum*. *European Journal of Protistology*, 46(2):143–9, 2010.

[43] D. W. Rogers, J. A. Denton, E. McConnell, and D. Greig. Experimental evolution of species recognition. *Current Biology*, 25(13):1753–1758, 2015.

[44] R. F. Hoekstra. On the asymmetry of sex: evolution of mating types in isogamous populations. *Journal of Theoretical Biology*, 98(3):427–451, 1982.

[45] J. R. Christie and M. Beekman. Selective sweeps of mitochondrial DNA can drive the evolution of uniparental inheritance. *Evolution*, 71(8):2090–2099, 2017.

[46] S. Geng, P. De Hoff, and J. G. Umen. Evolution of sexes from an ancestral mating-type specification pathway. *PLoS Biology*, 12:1–16, 2014.

[47] A. Menkis, D. J. Jacobson, T. Gustafsson, and H. Johannesson. The mating-type chromosome in the filamentous ascomycete *Neurospora tetrasperma* represents a model for early evolution of sex chromosomes. *PLoS Genetics*, 4(3):e1000030., 2008.

[48] Y. Tsuchikane, T. Fujii, M. Ito, and H. Sekimoto. A sex pheromone, protoplast release-inducing protein (PR-IP) inducer, induces sexual cell division and production of PR-IP in closterium. *Plant and Cell Physiology*, 46(9):1472–1476, 2005.

[49] P. Luporini, A. Vallesi, C. Miceli, and R. A. Bradshaw. Chemical signaling in ciliates. *The Journal of Eukaryotic Microbiology*, 42(3):208–12, 1995.

[50] G. W. A. Constable and H. Kokko. The rate of facultative sex governs the number of expected mating types in isogamous species. *Nature Ecology and Evolution*, 2(7):1168–1175, 2018.

[51] S. Vuilleumier, N. Alcala, and H. Niculita-Hirzel. Transitions from reproductive systems governed by two self-incompatible loci to one in fungi. *Evolution*, 67(2):501–516, 2013.

[52] Z. Hadjivasiliou, A. Pomiankowski, and B. Kuijper. The evolution of mating type switching. *Evolution*, 70(7):1569–1581, 2016.

[53] B. P. S. Nieuwenhuis and S. Immler. The evolution of mating-type switching for reproductive assurance. *BioEssays*, 38(11):1141–1149, 2016.

[54] B. P. S. Nieuwenhuis, S. Tusso, P. Bjerling, J. Stangberg, J. B. W. Wolf, and S. Immler. Repeated evolution of self-compatibility for reproductive assurance. *Nature Communications*, 9(1):1639, 2018.

5 Acknowledgements

This research was funded by an Engineering and Physical Sciences Research Council Fellowship (EP/L50488/) and HFSP Long Term Fellowship to ZH, and by grants from the Engineering and Physical Sciences Research Council (EP/F500351/1, EP/I017909/1, EP/K038656/1) and the Natural Environment Research Council (NE/R010579/1) to AP.

6 Figure legends

Figure 1

Gametes communicate through ligand and receptor molecules. The ligand can be either membrane bound or released in the local environment. (a) When the interacting cells produce ligand and receptor symmetrically, the ligand will bind to receptors on its own membrane as well as those on the other cell. This may impair intercellular signaling. (b) Producing the ligand and receptor in an asymmetric manner resolves this issue.

Figure 2

Signaling interactions between mating cells can be severely impaired due to ligand-receptor interactions in the same cell. (a) The amount of free ligand in individual cells at steady state $[L]^*$ and (b) normalized amount of free ligand at steady state $[L]^*/[L]_{max}$ varies with the intracellular binding rate k^+ and degradation rate γ. (c) The relative amount of incoming signal W_{12} for a cell that produces ligand and receptor asymmetrically versus symmetrically decreases with the degradation rate $\gamma$and weaker binding k^+. (d-f) The product of the incoming signal of two interacting cells $W_{12}W_{21}$ (determining the likelihood of a successful mating interaction) varies with ligand and receptor production rates in cell$_1$ and cell$_2$. Other parameters used in the simulations are given in the Supplemental Material.

Figure 3

Evolution of asymmetric signaling roles and self-incompatible mating types. (a) The evolution of signaling asymmetry ($s = 0$ no asymmetry, $s = 1$ full asymmetry) over time. Two steady states (E_1 and E_2) are found as described in the main text. (b) Production rates of individual cells in the population for the receptor-ligand pairs $L-R$ (black) and $l-r$ (red) at E_2. (c) Production rates for the two receptor types R and r for individual cells at E_2. (d) Steady state signaling asymmetry s^* against the intracellular binding rate k^+. (e) Threshold value of k^+, beyond which E_2 becomes

stable against E_1, plotted versus n (cost of self-binding). The relationship is shown for different values of k_b (strength of between cell signaling) relative to k^+/k^- (strength of within cell signaling) (f): The steady state value for s^*, plotted versus the initial value s_0 and k^+. Plots are averaged at the steady state over 20 repeats. s^* values away from 0 or 1 reflect stochastic outcomes where the population evolves to either E_1 or E_2. Other parameters used in simulations detail in the Supplemental Material.

Figure 4

Recombination impacts E_2. (a) The evolution of s (signaling asymmetry) over time given a fixed recombination rate $r = 0.1$. (b) Steady state ss^* varies with the recombination rate. (c-e) Production rates of individual cells in the population for receptor-ligand pairs $L-R$ (black) and $l-r$ (red) for recombination rates (c) $, r = 0.1$ (d) 0.2 and (e) > 0.3. (f) The steady state value for ss^*, given a recombination rate $r = 0.2$, plotted versus the initial $s$value s_0 and k^+ averaged over 20 repeats. s^* values away from 0 or 0.5 reflect a stochastic outcome. Other parameters used in simulations detail in the Supplemental Material.

Figure 5

The steady state recombination rate r^* co-evolves with the ligand and receptor production rates. (a) Averaged across the population, r^* varies with k^+ (within cell binding rate) and $n = 0, 1, 2$ (cost of self-binding). Evolution trajectories of s(orange) and r(blue) over time for (b) $k^+ = 10$, (c) $k^+ = 3$ and (d) $k^+ = 1$. The recombination rate r was allowed to evolve alone for 1000 generations, following which mutation at the ligand and receptor loci was introduced. Other parameters used in simulations are given in the Supplemental Material.

Supporting information: Evolution of the mating type locus with suppressed recombination

Zena Hadjivasiliou and Andrew Pomiankowski

1 Model and computational details

We model N cells so that each cell is individually characterized by a ligand locus $\mathcal{L}$ and a receptor locus $\mathcal{R}$. Two ligand genes determine the production rates for two ligand types l and L given by ν_l and ν_L. Similarly, two receptor genes determine the production rates for the two receptor types r and R given by ν_r and ν_L. The two ligand and receptor genes in our model could could arise from dublication followed by mutation that leaves two closely linked genes that code for different molecules. In our computational set-up each cell is associated with production rates ν_l, ν_L, ν_r and ν_R where we assume a normalised upper bound so that $\nu_l + \nu_L \leq 1$ and $\nu_r + \nu_R \leq 1$.

The program is initiated with $\nu_L = \nu_R = 1$ and $\nu_l = \nu_r = 0$ for all cells (with the exception of Fig. 3f and Fig. 4f). We introduce mutation so that the ligand and receptor production rates of individual cells mutate independently at rate μ. A mutation event at a production gene changes the production rate by an increment ϵ where $\epsilon \sim N(0, \sigma)$. Mutation events at the different genes l, L, r and R are independent of one another. If $\nu_l + \nu_L > 1$ or $\nu_l + \nu_L > 1$ the production rates are renormalised so their sum is capped at 1. If a mutation leads to a production rate below 0 or above 1 it is ignored and the production rate does not change.

We implement mating by randomly sampling individual cells. The probability that two cells mate is determined by their ligand and receptor production rates as defined in Eq. (9) in the main text. We assume that K takes a large value relative to $W_{12}W_{21}$ so that P is linear in $W_{12}W_{21}$. Because the absolute value for $W_{12}W_{21}$ varies greatly between parameter sets, and what we are interested in is the relative change in $W_{12}W_{21}$ when signaling levels change, we chose K to be equal to the maximum value $W_{12}W_{21}$ can take for a given choice of γ, k^+, k^- and k_b. Sampled cells that do not mate are returned to the pool of unmated cells. This process is repeated until $M = N/2$ cells have successfully mated. These are

sampled with replacement until the population returns to size N. We assume that a mutation-selection balance has been reached when the absolute change in s, defined in Eq. (10) in the main text, between time steps t_1 and t_2 is below $\epsilon = 10^{-5}$ across $t_2 - t_1 = 100$. Certain parameter sets resulted in noisy steady states and were terminated following a minimum of 10^5 generations. The simulation keeps track of all production rates for individual cells over time.

We implement recombination by considering a modifier $\mathcal{M}$ that lies between the ligand and receptor loci $\mathcal{L}$ and $\mathcal{R}$. For simplicity, we assume that $\mathcal{M}$ determines the physical distance between $\mathcal{L}$ and $\mathcal{R}$ so that the distances $\mathcal{L} - \mathcal{M}$ and $\mathcal{R} - \mathcal{M}$ are the same. The modifier $\mathcal{M}$ determines the rate of recombination quantitatively by determining r_M, the probability of a single recombination event following mating. Consider for example two individuals whose ligand and receptor production rates and recombination rate are determined by the triplets $R_1 - M_1 - L_1$ and $R_2 - M_2 - L_2$, the possible offspring resulting from such a mating are given by,

1. $R_1 - M_1 - L_1$ and $R_2 - M_2 - L_2$ with probability $(1 - r_{M_{1,2}})^2$ – equivalent to no recombination events

2. $R_1 - M_2 - L_1$ and $R_2 - M_1 - L_2$ with probability $r^2_{M_{1,2}}$ – equivalent to two recombination events

3. $R_1 - M_2 - L_2$ and $R_2 - M_1 - L_1$ with probability $r_{M_{1,2}}(1 - r_{M_{1,2}})$ – equivalent to one recombination event

4. $R_1 - M_1 - L_2$ and $R_2 - M_2 - L_1$ with probability $r_{M_{1,2}}(1 - r_{M_{1,2}})$ – equivalent to one recombination event

where $r_{M_{1,2}} = \frac{1}{2}(r_{M_1} + r_{M_2})$.

We allow mutation in the recombination locus at rate μ_r independently of the ligand and receptor loci. A mutation event leads to a new recombination rate so that $r'_M = r_M - \epsilon$ for $\epsilon \sim N(0, \sigma_r)$. We assume that the mutation-selection balance has been reached when the absolute change in s, defined in Eq. (10) in the main text, and the change in the average recombination rate between time steps t_1 and t_2 is below $\epsilon = 10^{-5}$ across $t_2 - t_1 = 100$.

2 Methods and parameters used for main text figures

Fig. 3

(a): Individual simulations following the trajectory of s over time. Population is initiated at $(\nu_L, \nu_R, \nu_l, \nu_r) = (1,\ 1,\ 0,\ 0)$ and $r = 0$ for all cells at time 0. $\mu = 0.01$ for all ligand and receptor genes and $\mu_r = 0$. $\sigma = 0.1$, $\gamma = 0.5$, $k^- = 1$, $n = 1$, $k_b = k^+/k^-$. $k^+ = 1.0$ for E_1 trajectory and 1.0 for E_2 trajectory. Population size $N = 1000$ and number of cells allowed to mate $M = N/2$.

(b-c): Parameters as for (a) with $k^+ = 5.0$. Each dot is represents an individual cell in the simulation.

(d): Parameters used as for (a) with varying k^+ and γ as indicated in the figure. Simulation was run until a steady state was reached and the value of s^* was averaged over the last 1000 time steps to account for noise.

(e): Parameters used as for (a), varying k_b and n as indicated in the figure. k^+ was also varied here and the value of k^+ beyond which E_2 became stable at the expense of E_1 was noted (the y-axis value).

(f): Parameters as for (a) but varying k^+ and initial conditions as shown in the figure. Initial conditions were set to $(\nu_L, \nu_R, \nu_l, \nu_r) = (1-\delta, 1, \delta, 0)$ for half of the population and $(1, 1-\delta, 0, \delta,)$ for the other half where the value of δ is reflected in the value for s_0. The heat maps show the value of s^* at steady state averaged over 20 repeats.

Fig. 4

(a): Individual simulations following the trajectory of s over time. Population is initiated at $(\nu_L, \nu_R\ , \nu_l, \nu_r) = (1,\ 1,\ 0,\ 0)$ and $r = 0.1$ for all cells at time 0. $\mu = 0.01$ for all ligand and receptor genes and $\mu_r = 0$. $\sigma = 0.1$, $\gamma = 0.5$, $k^- = 1$, $n = 1$, $k_b = k^+/k^-$. $k^+ = 1.0$ for E_1 trajectory and 1.0 for E_2 trajectory. Population size $N = 1000$ and number of cells allowed to mate $M = N/2$.

(b): Parameters as in (a) but varying r as indicated in the figure and using $k^+ = 3.0$. The y axis shows the steady state value of s averaged over 1000 steps after steady state has been reached.

(c-e): Parameters as for (a) with $k^+ = 5.0$ and recombination rate r as shown in each figure. Each dot is represents an individual cell in the simulation.

(f): Parameters as for (a) but varying k^+ and initial conditions as shown in the figure. Initial conditions were set to $(\nu_L, \nu_R,\ \nu_l, \nu_r) = (1-\delta, 1, \delta, 0)$ for half of the population and $(1, 1-\delta, 0, \delta,)$ for the other half where the value of δ is reflected in the value for s_0. The heat maps show the value of s^* at steady state averaged over 20 repeats.

Fig. 5

(a): Population is initiated at $(\nu_L, \nu_R\ ,\ \nu_l, \nu_r) = (1,\ 1,\ 0,\ 0)$ and $r = 0.0$ for all cells at time 0. $\mu = 0.01$ for all ligand and receptor genes and $\mu_r = 0.01$. $\sigma = \sigma_r 0.1$, $\gamma = 0.5$, $k^- = 1$, $k_b = k^+/k^-$. k^+ and n vary as shown in the plot. The y axis shows the steady state value of r averaged over 1000 steps after steady state has been reached. Population size $N = 1000$ and number of cells allowed to mate $M = N/2$.

(b-d): Parameters as in (a) with k^+ varied as shown in the individual plots.

3 Supplementary figures referenced in the main text

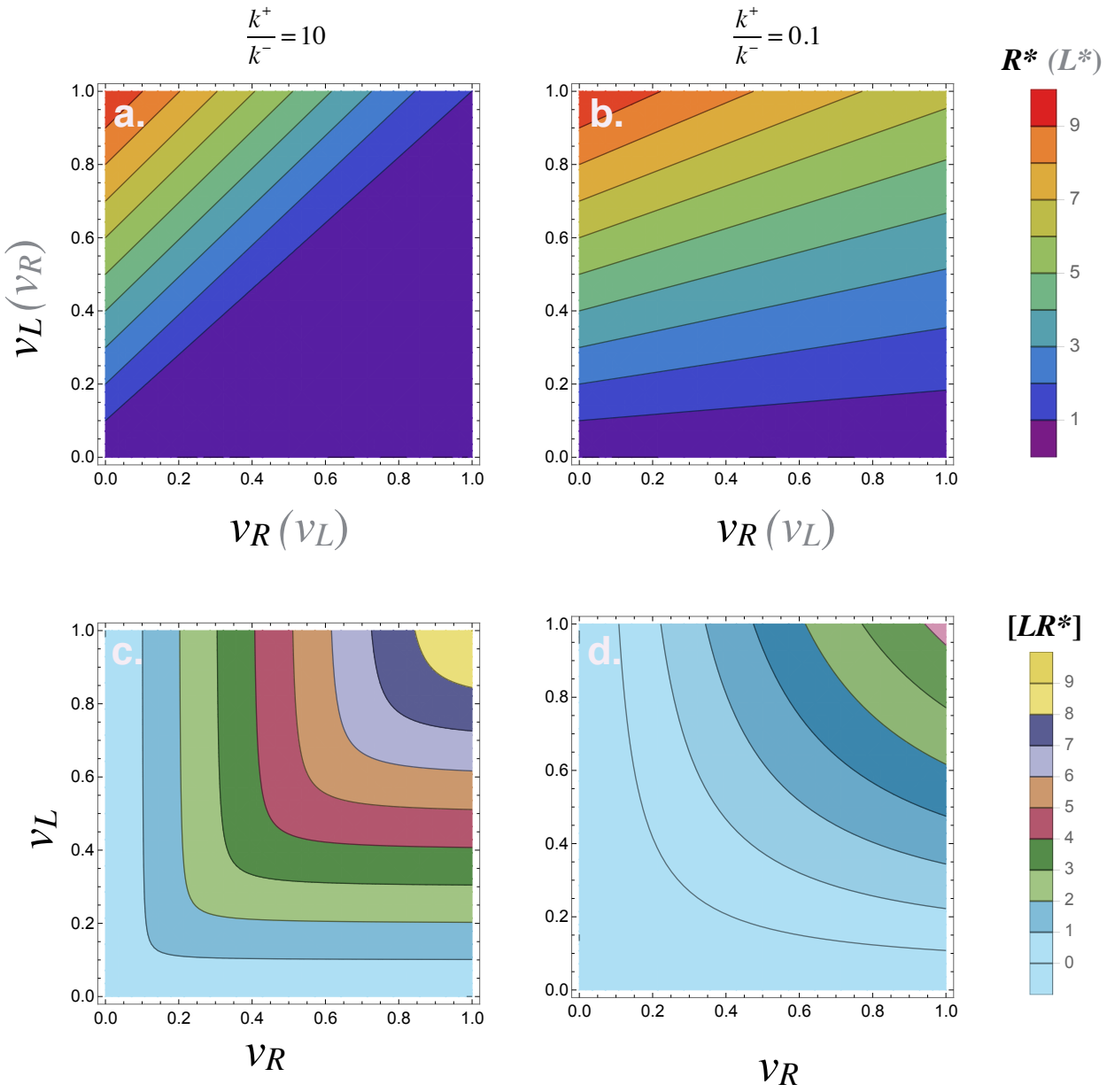

Figure S5: **Steady state concentrations in individual cells** Steady state concentration of the ligand L and receptor R in individual cells when varying the ligand and receptor production rates ν_L and ν_R for $k^+/k^- = 10$ (a) and $k^+/k^- = 01$ (b). (c-d) show the concentration of ligand-receptor complexes for the same parameter variations. Other parameters used: $\gamma_R = \gamma_L = \gamma_{LR} = 0.1s^{-1}$

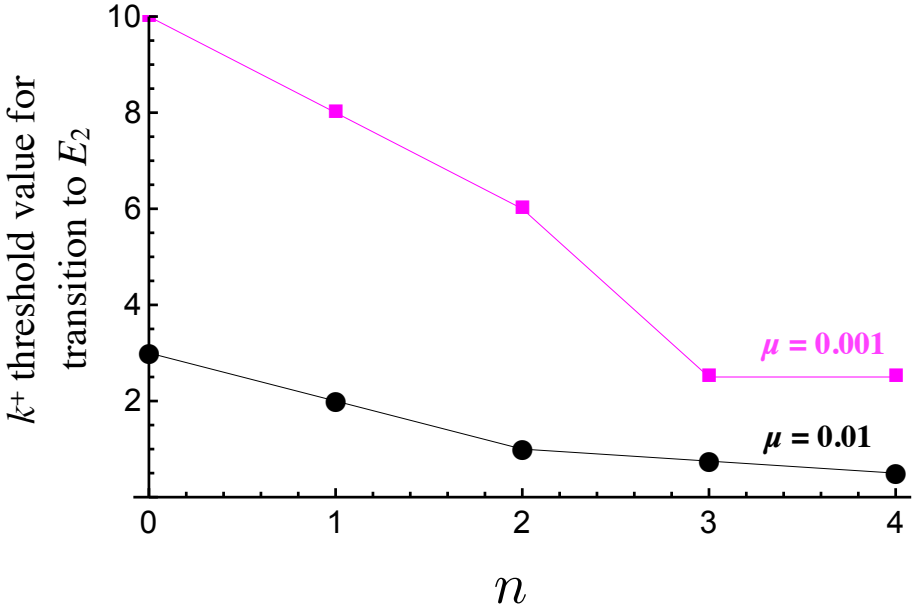

Figure S6: **The role of mutation rates.** The threshold value of k^+, beyond which E_2 becomes stable against E_1, plotted versus n which dictates the cost of self-binding for $\mu = 0.1$ and $\mu = 0.001$ to show that lower mutation rates require more stringent conditions for the evolution of signaling asymmetry. Population is initiated at $(\nu_L, \nu_R, \nu_l, \nu_r) = (1, 1, 0, 0)$ and $r = 0$ for all cells at time 0. $\mu = 0.01$ for all ligand and receptor genes and $\mu_r = 0$. $\sigma = 0.1$, $\gamma = 0.5$, $k^- = 1$, $k_b = k^+/k^-$. $k^+ = 1.0$ for E_1 trajectory and 1.0 for E_2 trajectory. Population size $N = 1000$ and number of cells allowed to mate $M = N/2$